

# Experimental and Numerical Study on Disc-RDE: Flow Structure and its Performances

A, Koichi Hayashi<sup>1</sup>

*Aoyama Gakuin University, Shibuya, Tokyo 150-8366, Japan*

Kazuhiro Ishii<sup>2</sup>,

*Yokohama National University, Yokohama, Kanagawa 240-8501, Japan*

Tomohiro Watanabe<sup>3</sup>, Nobuyuki Tsuboi<sup>4</sup>, Kohei Ozawa<sup>5</sup>, Nicola H. Jourdain<sup>6</sup>

*Kyushu Institute of Technology, Kitakyushu, Fukuoka 804-8550, Japan*

Edyta Dzieminska<sup>7</sup> and Xinmeng Tang<sup>8</sup>

*Sophia University, Chiyoda, Tokyo 102-8554, Japan*

Tetsuro Obara<sup>9</sup> and Shinichi Maeda<sup>10</sup>

*Saitama University, Saitama, Saitama 338-8570, Japan*

Toshiharu Mizukaki<sup>11</sup>

*Tokai University, Hiratsuka, Kanagawa 259-1292, Japan*

**The present study discusses disc-type rotating detonation engine (DRDE) experimentally and numerically. The experimental work shows that the detonation propagates in three different modes; single, dual, and hybrid. The operating frequency of dual-wave mode is 1.8-2.1 times faster than that of single wave mode. The number of detonation wave can be predicted based on the pressure history and the operating frequency signal. The numerical work shows the performance of 3D numerical analysis of DRDE with uniform injection case and multiport injection case. By increasing the wave number from one to two, the detonation propagation velocity decreases by 18.7 %. The one-detonation head case gives some better performance to the flow than the two-detonation head case. The inlet flow angle to the radial turbine becomes about 50 degrees to the radial direction no matter how large the plenum chamber is.**

---

<sup>1</sup> Professor Emeritus, Ph.D., Department of Mechanical Engineering, Senior Member AIAA.

<sup>2</sup> Professor, Dr., Department of Mechanical Engineering, Non-Member AIAA.

<sup>3</sup> Graduate Student., Mr., Department of Mechanical and Control Engineering, Non-Member AIAA.

<sup>4</sup> Professor, Dr., Department of Mechanical and Control Engineering, Senior Member AIAA.

<sup>5</sup> Assistant Professor, Dr., Department of Mechanical and Control Engineering, Member AIAA.

<sup>6</sup> Graduate Student., Mr., Department of Mechanical and Control Engineering, Non-Member AIAA.

<sup>7</sup> Associate Professor, Dr., Department of Engineering and Applied Sciences, Faculty of Science and Technology, Non-Member AIAA.

<sup>8</sup> Researcher, Dr., Department of Engineering and Applied Sciences, Faculty of Science and Technology, Non-Member AIAA.

<sup>9</sup> Professor, Dr., Graduate School of Science and Engineering, Saitama University  
255 Shimo-Okubo, Sakura-ku, Saitama-shi, Saitama 338-8570, Japan, Non-Member AIAA.

<sup>10</sup> Assistant Professor, Dr., Graduate School of Science and Engineering, Saitama University, Member

<sup>11</sup> Professor, Dr., Department of Aeronautics and Astronautics-Aerospace course,

## I. Introduction

Hint of disc type rotating detonation engine (RDE) was given by Nakagawa et al. (2017)[1] of Kasahara's group, who were trying to visualize a standard RDE detonation structure to see its dynamics in an ethylene/oxygen mixture. Then they cut the size of their standard RDE shorter like a disc shaped RDE to see the rotating part of detonation clearer to avoid its three-dimensional effect. They could see the clearer injection jet structure and rotating detonation interaction well, but not in detail. Their average detonation speed was about 1600 m/s for  $C_2H_4/O_2$  mixture at the equivalence ratio of 1.6.

At the almost same time with the Kasahara group's development of disc-like RDE, USAFRL/ISSI did perform a RDE experiment on the open-loop of real gas turbine engine (P63GTE) (Naples et al. ,2017 [2]) . They studied good or bad of the combination between RDE and GTE, and obtained the result after 20 min run that the performance of RDE-GTE was reasonable or probably better than that of GTE alone.

Later since its exhaust gas flows out near the center axis and it can be made more compact than standard RDE, the USAFRL group started to study radial-RDE (RRDE) or disc-RDE (DRDE) extensively. Huff et al. (2018) [3] pointed out the characteristics of RDE are generally (1) high combustor exit pressure, (2) compact design, (3) high combustion efficiency, (4) large work, and desined disc-RDE to run eight times and to get about 70 % of CJ detonation speed. They wanted to see whether the RRDE performance is better than that of standard RDE. McClearn et al. (2018) [4] investigated probably first time in the world the performance of the RRDE designed by Huff et al. [3] and connected with a radial inflow turbine. They did not find any serious damage when they run connecting with the radial inflow turbine to obtain the increase of power per round. They also found that the mass flow rate increases at the maximum power, but knew there is a limit of mass flow rate. However they said the RRDE has a good future and must be checked their performance further. Then Huff et al. (2018) [5] studied the performance of their RRDE coupled with a bleed air turbine to confirm that its power increases as its rotation increases. Again they promised the future of their RRDE.

Last year (2019) the flow visualization experiment in RRDE was presented by Boller et al. (2019) [6] of AFRL to show how the detonation wave propagates in radial direction. Their RRDE has one or two detonation waves (DW) : the one-DW is unstable basically to move between the inner nozzle edge and outer wall, the DW becomes stable when it is in the two-DW mode. These phenomena were confirmed visually. As for turbine connection, the flow from RRDE to turbine is affected by the change of DW and give a possible damage to the turbine.

Then Huff et al. (2019) [7] said about the usefulness of RRDE for a compact rapid response power generator in aircraft that a coupling between RRDE and GTE is an answer for such case. In their paper the relation between the geometry of RRDE and detonation mode and the performance of GTE with RRDE are discussed.

At 2020 AIAA SciTech meeting, the Japanese RDE-GTE group (Hayashi et al. [8]) presented a preliminary DRDE study. The numerical study of a 3-D DDRE performance with a  $H_2/O_2$  mixture showed that the detonation velocity becomes higher than C-J values when the initial stagnation injection pressures are 0.5~1.0 MPa, which is different from the experiment described below. We also found that the flow angle to the radial direction was anout 50 degrees. One-DW and two-DW cases were simulated to find that two-DW case gradually became one-DW time. In all simulations we did not calculate any back flow at injection.

Paxson (2020) [10] also did calculate a DDRE using the quasi-2D, two-species, reactive Euler equations without inlet back flow and it turned out that DW sticked to the inner wall as well as the outer wall. Their detonation speed was faster at the inward case than C-J detonation value and slower at the outward case.

Muraleetharan et al. (2020) [11] used a constant hight geometry of RRDE chamber section to compre that with the constant area geometry chamber which is popular. They found that the constant hight geometry chamber provides the reduction of the pressure loss created by expansion fans on both radial sides of the DW.

At the present presentation our experimental work done by Ishii's group will show the visualization for of the single-wave mode , dual-wave mode, and hybrid-wave mode, operating frequency of DW, pressure history, and operating frequency by DFT spectrum of detonation propagation for DRDE. The 3D numerical simulations are performed by Tsuboi's group to show the visualization of DRDE detailed flow structure and the effect of flow field characteristics on the DRDE performance. Especially the uniform fuel and oxidizer injection using the 3D Euler equations and multiple-injection system cases using 3D Navier-Stokes equations will be discussed.

## II. Experiments

The DDRE system for the experimental study is shown in Fig.1 and its mixture supply system is shown in Fig.2.

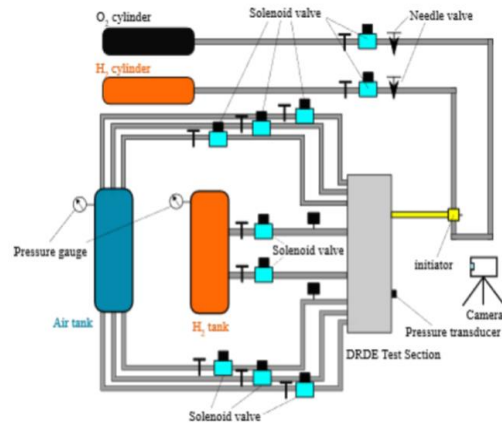
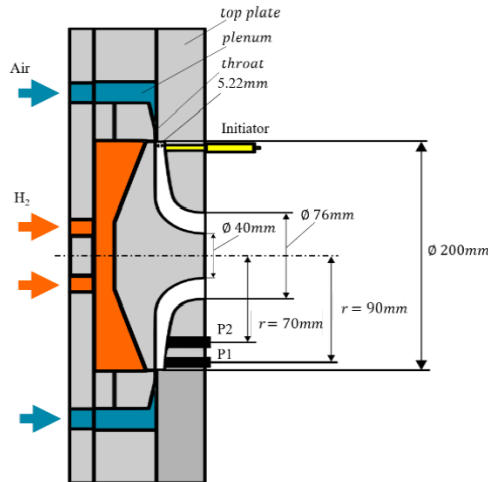


Fig. 1 Schematic diagram of the DRDE combustion Fig. 2 Mixture supply system of the present DRDE

The whole system schematic diagram used last year is shown in Fig.1 and its mixture supply system is shown in Fig.2. This time the experiments were performed with the new top plate (Figs.3 and 4) which is a little different from the last year's one (Fig.1) and has an acrylic glass for visualization. Reactant gases (both H<sub>2</sub> and air) flow from the combustion chamber circumference to the radial direction, burn by rotating detonations, and come out to the center direction. The flow channel cross section is planned to be constant along the gas flow pass (the constant area geometry [11]).

As shown in Figs.1 and 2, fuel is hydrogen and is supplied by 120 orifice holes of 0.51 mm in diameter, which are located at circumferential direction. Oxidiser is air and is supplied from the circumference through slits distributed circumferentially. Hydrogen and air jets are collided each other at 90 degrees to get uniform mixtures. After both jets collided, they flow into the combustion chamber. The detonation is initiated by an initiator tube installed near the circumference of combustion chamber. A stoichiometric H<sub>2</sub>/O<sub>2</sub> mixture is filled before hand and is ignited by a spark plug at this small tube end to send off detonation to the combustion chamber. The behavior of rotating detonation in the combustion chamber is grasped by two pressure gauges of P1 and P2 (Kisler 603B1) which are located at the wall of the combustion chamber (see Fig.1).

Figure 2 shows the mixture supply system. Hydrogen and air are stored in the tanks in advance, then are provided into the combustion chamber through the several pipes. Table 1 shows the supply time of each gas is controlled by a solenoid valve and is 226 ms considering the tank volume, mass flow rate, and equivalence ratio.

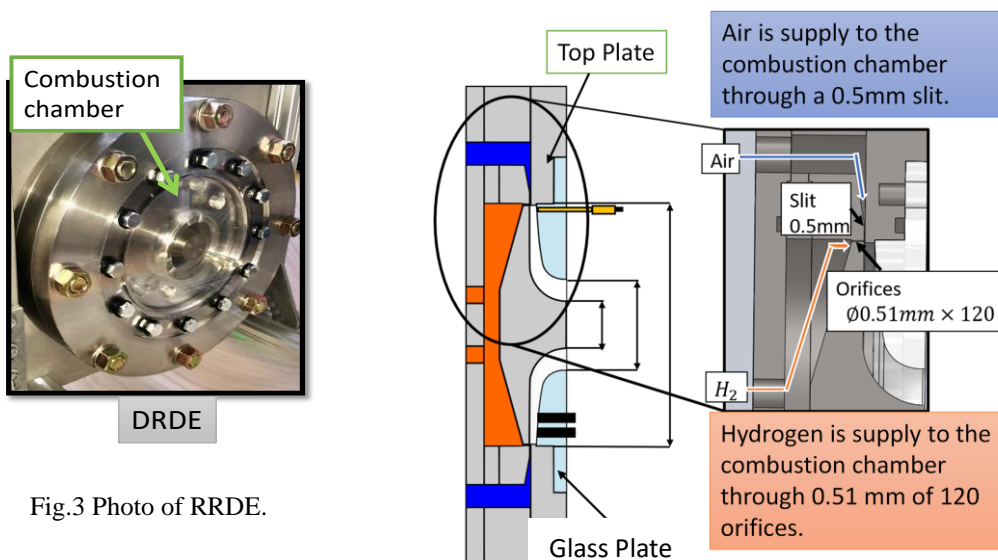


Fig.3 Photo of RRDE.

Fig. 4 Schematics of the DRDE with the glass plate.

Table 1 Test running time, mass flow rate, and equivalence ratio.

Test running time	226ms
Mass flow rate	$290 \pm 10\text{g/s}$
Equivalence Ratio	0.55 ~ 1.45

Table 2 Test gas and its supply method for DRDE and initiator.

	DRDE	Initiator
Test gas	$H_2$ and AIR	$H_2 - O_2$
Supply method	Gases are temporarily store in tank. (Direct supply from the cylinder cause insufficient of mass flow rate)	Direct supply from the cylinder.

Table 2 shows the mixtures and their supply methods for DRDE and the initiator. As shown in Fig.2, The test flow rate of hydrogen and air needs a sufficient amount, hence the hydrogen and air tanks for the DRDE are much larger than that for the initiator.

The visualization system with the high speed camera of NAC (MEMRECAM High Speed Camera Series) is shown in Fig.5. The framing speed are  $3.0 \times 10^4$  and  $4.0 \times 10^4$ . This high speed camera covers the entire combustion chamber field. The dump tank in Fig.5 is for sucking the high pressure exhaust gases to keep the test room at low pressure. The test room works as a pressure holder, a sound absorber and a explosion protector.

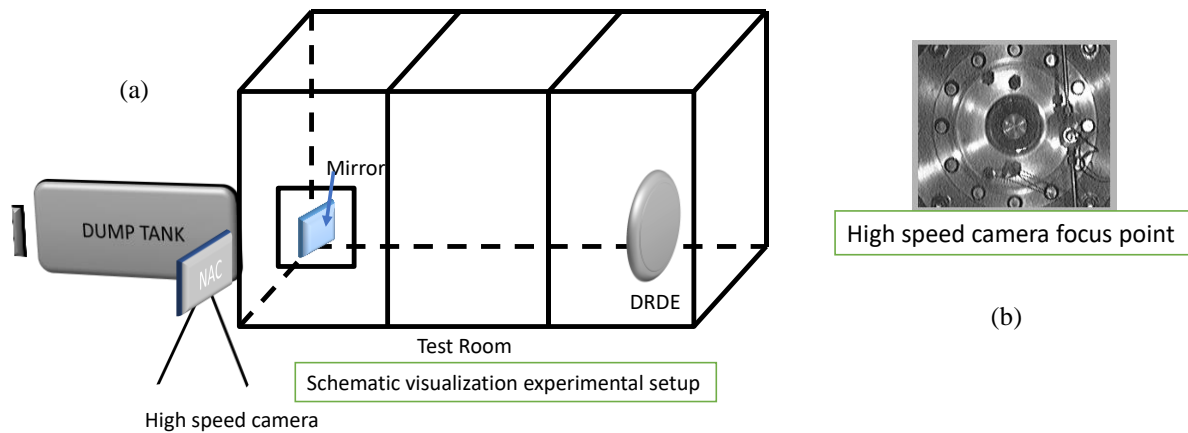


Fig. 5 Schematic configuration of visuarization set up: (a) the wjhole view, (b) the high speed camera focused photo.

### A. High speed camera photo: Single detonation wave mode

The result of high speed camera photo for the single detonation wave mode case is shown in Fig.6. This case is obtained at the total mass flow rate of 296 g/s and at the equivalence ratio of 0.767. The frame speed of the high speed camera was 30000 f/s. The detonation wave rotated at the counter clockwise direction along the outer edge of the DRDE combustion chamber. The expansion fan was appeared to tilte upward and to move away from the DW. We also recognized the chemiluminescence of the reflected wave from the inner wall.

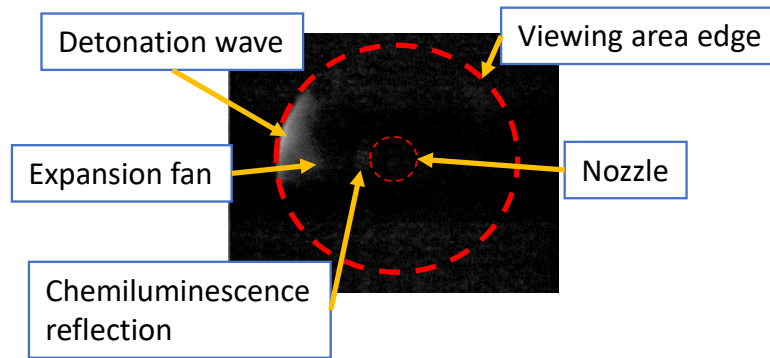


Fig. 6 Detonation wave propagation structure; Single DW mode.

### B. High speed camera photo: Dual detonation wave mode

The result of high speed camera photo for the dual detonation wave mode case is shown in Fig.7. This case is obtained at the total mass flow rate of 298 g/s and at the equivalence ratio of 0.841. The frame speed of the high speed camera was 30000 f/s. Two detonation waves rotated at the clockwise direction along the outer edge of the DRDE combustion chamber. However the blightness of DWs is less than the case of single DW mode. The expansion fan was not seen for this case. But DW is more stable than that at the case of single DW mode.

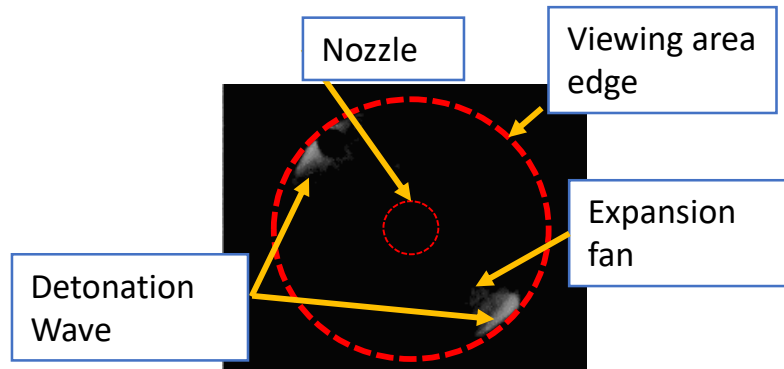


Fig. 7 Detonation wave propagation structure; Dual DW mode.

### C. High speed camera photo: Hybrid detonation wave mode

The result of high speed camera photo for the hybrid detonation wave mode case is shown in Fig.8. This case is obtained at the total mass flow rate of 290 g/s and at the equivalence ratio of 1.45. The frame speed of the high speed camera was 40000 f/s. This case has a single and a dual DW which coexist and rotate in clockwise direction at the first time and later rotate in counter-clockwise direction to become stable along the outer edge of the DRDE combustion chamber. The expansion fan was not seen in this case too. The mode shift from clockwise rotation to counter-clockwise rotation takes 80 ms.

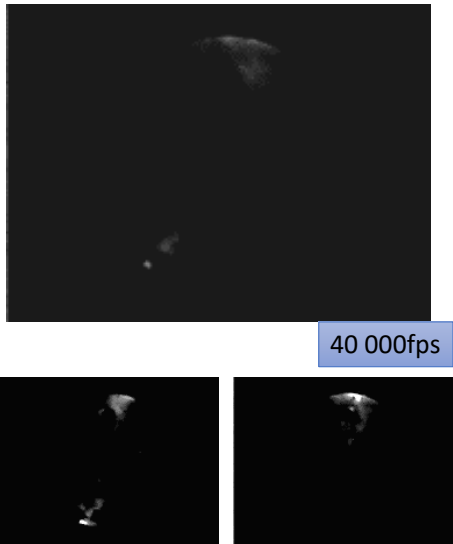


Fig. 8 Detonation wave propagation structure; Hybrid DW mode.

**D. Discrete Fourier Transform for DRDE**

We used the discrete fourier transform (DFT) to find out the dominant frequency of DRDE. Figure 9 is the frequency profiles for DRDE DW rotation mode where (a) is the single DW mode, (b) the dual DW mode, and (c) the hybrid DW mode. The x-axis of the frequency profile is time, the y-axis is the frequency, and z-axis is the spectrum intensity. We obtained the dominant frequency of the single DW mode is 3.4 kHz, that of the dual DW mode is 6.1 kHz, and that of the hybrid DW mode is 3.2 kHz for the single DW and 6.4 kHz for the dual DW mode. The relation between the frequency and the equivalence ratio of mixture is described in Fig. 10.

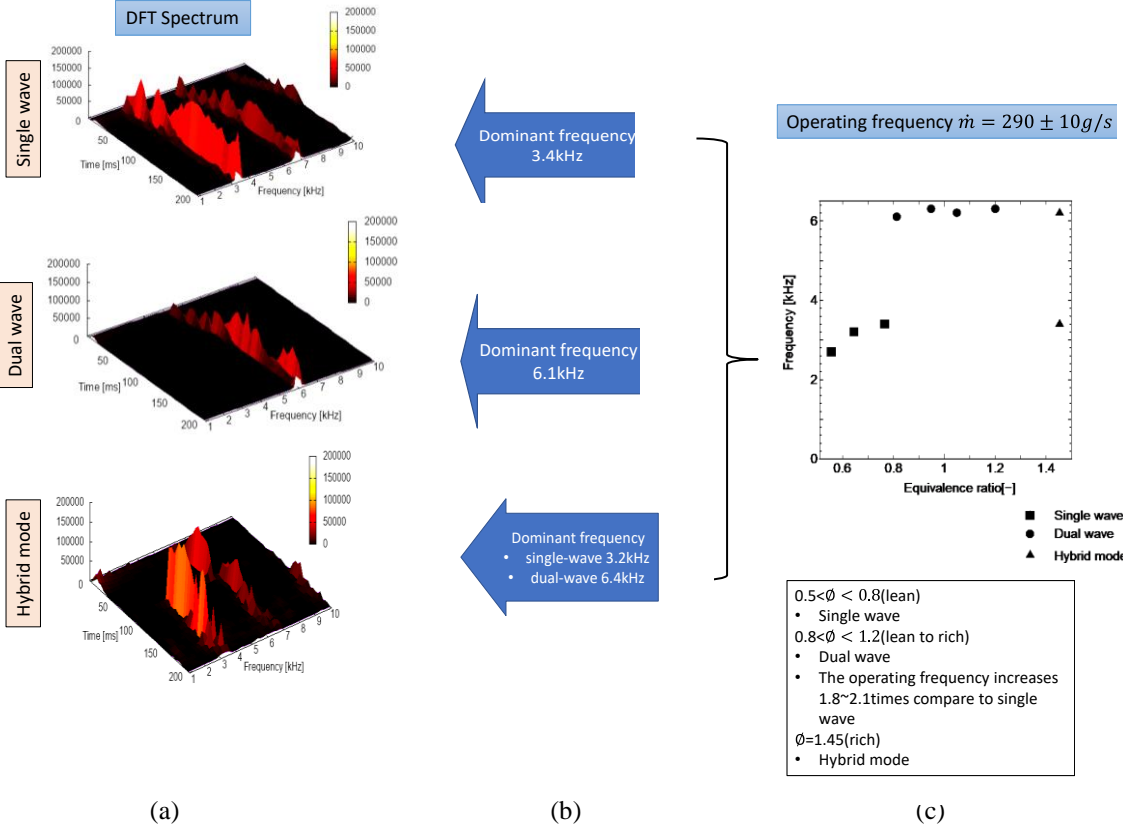


Fig. 9 Dominant frequency of DRDE based on DFT.

### E. Pressure histories of DRDE from pressure transducer near the injection

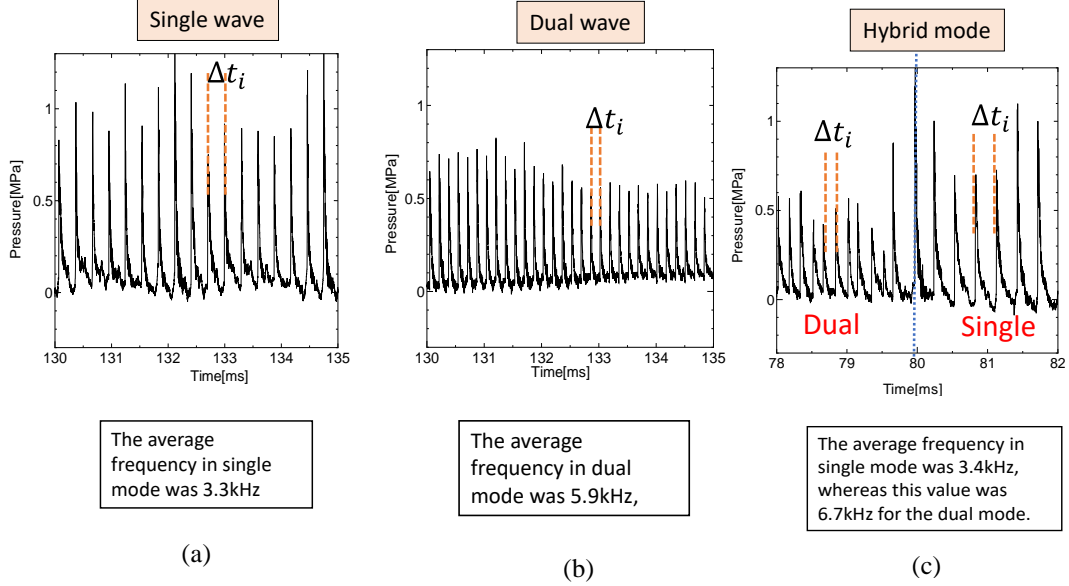


Fig. 10 Pressure time-history profiles of DRDE: (a) single DW mode, (b) dual DW mode, and (c) hybrid DW mode.

The pressure histories are obtained using the pressure transducer near the injection. We can find the average frequency of the detonation in DRDE. The average frequency is calculated from the following Eq. (1):

$$\bar{f} = \sum_i^N \frac{f_i}{N} \quad (1)$$

where  $i$  is the time interval. The average frequency of the single DW mode was 3.3 kHz, that of the dual DW mode was 5.9 kHz, and that of the single DW mode in the hybrid DW mode was 3.4 kHz and that of the dual DW mode in the hybrid DW mode was 6.7 kHz. The pressure time-history profiles are shown in Fig.10 for (a) the single DW mode, (b) the dual DW mode, and (c) the hybrid DW mode. From these pressure history, the dual DW mode looks more stable than the other two DW modes. From the experimental results for stability, the uniform pressure peak can be achieved by balancing the pressure in the combustion chamber and by increasing the wave number from the comparison between the single DW mode and the dual DW mode. In many standard RDE experiments, we know the higher wave number provides the better stability.

### F. Conclusion

The followings are obtained as a conclusion:

- (1) Detonation wave propagates along the outer diameter of combustion chamber.
- (2) At the constant mass flow rate  $\dot{m} = 290 \pm 10 g/s$  under 0.55 to 1.45 range of the equivalence ratio, the detonation propagates in three different modes; single, dual, and hybrid.
- (3) The operating frequency of dual-wave mode is 1.8~2.1 times faster than that of single wave mode.
- (4) The number of detonation wave can be predicted based on the pressure history and the operating frequency signal.

### III. Numerical Analyses

#### A. Numerical method

The three-dimensional compressible Euler equations with 9 species and 21 reactions and with an uniform injection system as well as the three-dimensional compressive Navier-Stokes equations with 9 species and 21 reactions and with a multi ignition system are used as the governing equations. A semi-implicit method for source terms and explicit way for the other terms are applied. The numerical flux in the convection term uses AUSMDV [12] with the second-order MUSCL and minmod limiter. The integration of the source term applies for the point implicit method. The time integration uses three-stage TVD Runge-Kutta method. The UT-JAXA [13] reaction model with nine species and twenty one chemical reactions are used for the detailed chemical reaction mechanism, which is good for not only high temperature but also high pressure combustion.

#### B. Computational details

##### [Uniform injection system]

Figure 11 shows the numerical injection system which is used for the uniform injection way. present computational grid system. The present DRDE is used by Hoff et al. [3]. The results of 1D detonation is used as an ignition source to start 3D DRDE calculation. The micro-nozzles are set at all outer circumference region. The amount of the injected gaseous mixture is controlled by the nozzle area ratio,  $A_e/A_t$ . The injection of the mixture is supersonic. Because the supersonic air inlet comes out due to the high pressure in the combustion chamber, two

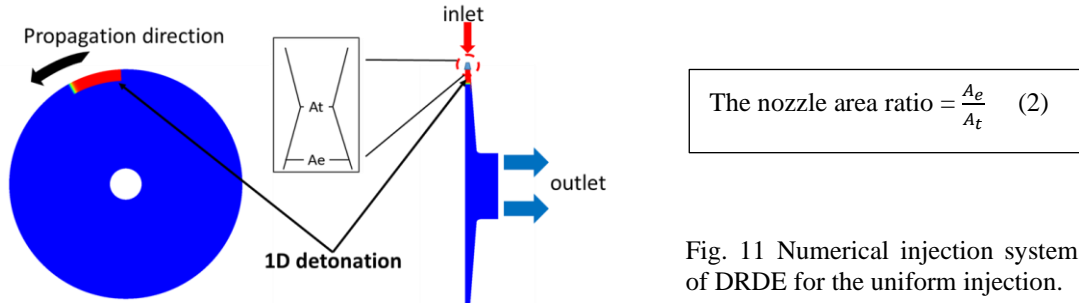
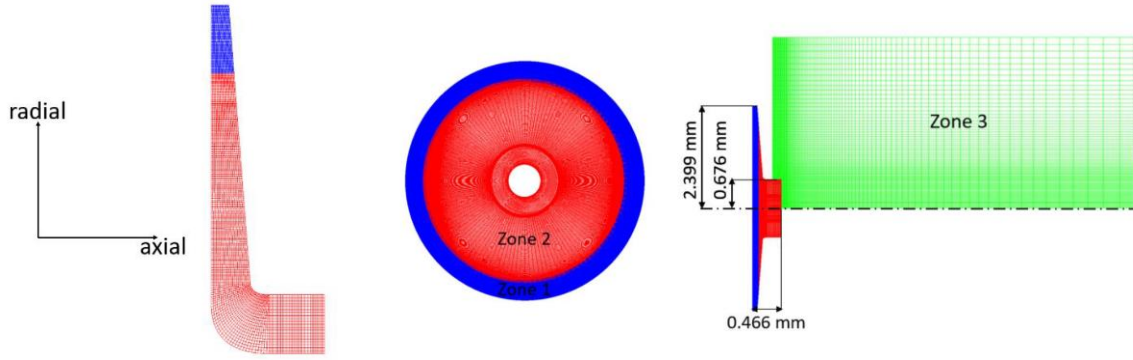


Fig. 11 Numerical injection system of DRDE for the uniform injection.

boundary condition systems, supersonic and subsonic, are used for the injection of the  $H_2/O_2$  mixture. The following four-step system developed by Zhdan et al. [14] is used this time:

- (1) If the inlet pressure is higher than the nozzle pressure, the pressure is extrapolated and the speed sets to zero.
- (2) If the pressure at the inlet is lower than the nozzle pressure and higher than the pressure behind the inlet, the pressure is extrapolated.
- (3) If the inlet pressure is between the supersonic condition and the subsonic condition, the pressure is extrapolated.
- (4) If the inlet pressure is very low, gas accelerates in the expansion region of the nozzle and the injection speed is supersonic.

The grid system is that the three-dimensional region is divided by three numerical zones (Fig. 12). Table 3 provides the number of the grid points for the three zones and the total grid numbers. The grid number of the dimension is (radial number) $\times$ (axial number) $\times$ (circumferential number). The connection of different grids is provided by interpolation coefficients. The mesh is made fine in the detonation propagation zone (Zone 1). The minimum grid size is 2.5  $\mu m$  in the radial direction of the zones 1 and 2. In the present study the flow field inside the combustion chamber is calculated in Zones 1 and 2 and the flow field behind the exit is calculated in zone 3.



(a) The grid system of zones 1 and 2

(b) The grid system of zone 2

(c) The grid system of zones 2 and 3

Fig. 12 Computational grid system: (a) zones 1 and 2, (b) zone 2, and (c) zones 2 and 3.

Table 3 The computational grids for the uniform injection system

	Zone 1	Zone 2	Zone 3
Grid point ( $i \times j \times k$ )	81x21x601	204x21x131	110x99x71
Total grid points	2245000		

The numerical condition is that the injection mixture of  $H_2/O_2$  is stoichiometric; initial air temperature is 300 K and initial air pressure is 0.1 MPa; The micro-nozzle area ratio to the nozzle throat  $A_e/A_t$  is 5.0; the stagnation pressure is set to a low value of 0.5 MPa.

**[Multiport injection system]**

The multiport injection system is also applied to see the difference between the uniform injection and the multiport injection where the number of injection ports is 45 this time.

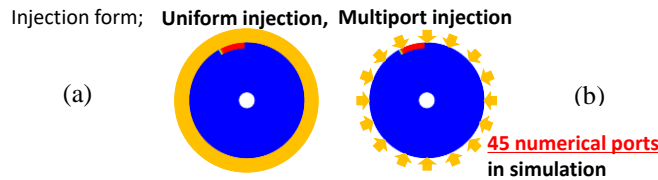


Fig. 13 The two-injection system: (a) uniform injection system and (b) multiport injection system.

**[Initial conditions]**

The initial condition for this DRDE simulations is described in Table 4.

Table 4 The initial conditions for both the uniform injection system and multiport injection system

	① Stagnation pressure comparison	② Number of wave comparison
Mixture gas	$H_2/O_2$	$H_2/O_2$
Number of detonation wave	1-wave	1-wave, 2-wave
Governing equation	Euler equations	Euler equations, Navier-Stokes equations (injection position)
Injection form	Uniform injection	Multiport injection
Micro nozzle area ratio	5.0	5.0
Stagnation pressure (Pst)	0.5, 0.8, 1.0 MPa	0.5 MPa
Stagnation temperature	300 K	300 K
Equivalence ratio	1.0	1.0

**C. Results and discussion for numerical simulation**

The main study for DRDE this time is (1) the characteristics of the internal flow field and the effect of the plenum pressure on the internal flow field; and (2) the characteristics of the internal flow field for two-detonation wave case. But first of all, the difference of detonation structure between using the uniform injection system and using the multiport injection system.

**[Uniform injection and multiport injection]**

The present study will first show the difference between the uniform injection system and as Fig.14 shows the unburned region is larger for the uniform injection case than that for the multiport injection system. Hence the multiport injection system which is closer to the real case will give the unstable condition for DRDE system. Fig. 15

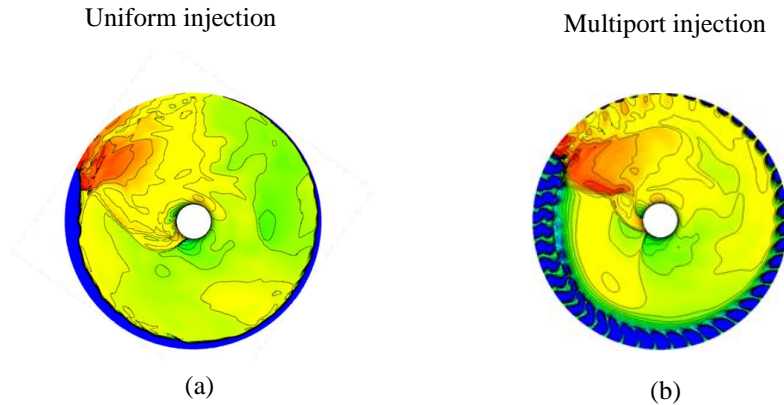


Fig. 14 The comparison of flow field using (a) the uniform injection system and (b) the multiport injection system.

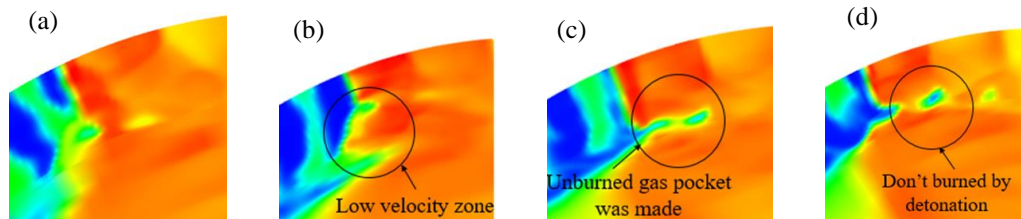
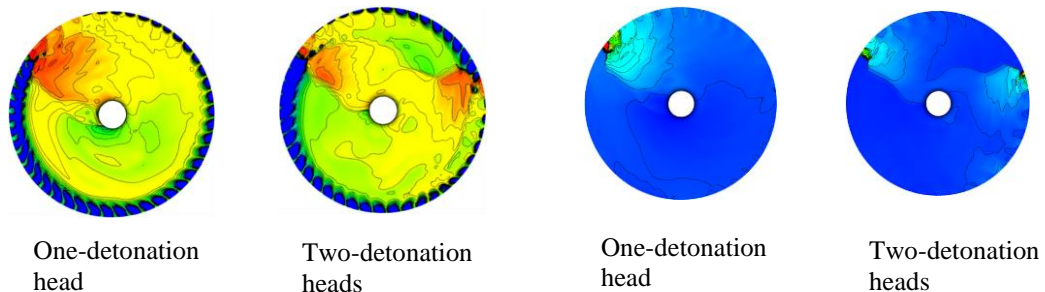


Fig. 15 The detonation structure using the multiport injection system: all have the unreacted pockets. shows the case using the multiport injection system. The detonation structure gradually collapses by non-reacted pockets appearance. This is a typical detonation failour case. As far as the detonation propagation velocity, the propagation velocity (3014 m/s) of the multiport injection case provided 3.3 % less velocity than that for the uniform injection case (3118 m/s).

**[The effect of wave number on the detonation propagation velocity]**

The effect of the wave number on the detonation propagation velocity was studied and the one detonation head case has fater propagation velocity (3014 m/s) than that with two-detonation head case. Figure 16 shows the temperature and pressure comparison between the one-detonation case and two-detonation case.





- [2] A.G. Naples, J.L. Hoke, R.T. Battelle, M. Wagner, F.R. Schauer, "RDE Implementation into an Open-Loop T63 Gas Turbine Engine," 55<sup>th</sup> AIAA Aerospace Science Meeting, AIAA 2017-1747 (2017). Doi: 10.2514/6.2017-1747.
- [3] Huff, R., Polanka, M. D., McClearn, M. J., Schauer, F. R., Fotia, M. L., and Hoke, J. L., "A Disk Rotating Detonation Engine Part 1: Design and Buildup," *2018 AIAA Aerospace Sciences Meeting*, AIAA Paper 2018-0633, Kissimmee, Florida, 2018. Doi:10.2514/6.2018-0633.
- [4] M. J. McClearn, F. R. Schauer, R. Huff, M. Polanka, J. L. Hoke, M. Fotia, "A Disk Rotating Detonation Engine Part 2: Operation," AIAA Paper 2018-1607 (2018). Doi: 10.2514/6.2018-1607.
- [5] R.T. Huff, M.D. Polanka, M.J. McClearn, F.R. Schauer, M.L. Fotia, J.L. Hoke, "A Radial Rotating Engine Driven Bleed Air Turbine," AIAA 2018-4879 (2018). Doi: 10.2514/6.2018-4879.
- [6] S.A. Boller, M.D. Polanka, R. Huff, F. Schauer, M. Fotia, J. Hoke, "Experimental Flow Visualization in a Radial Rotating Detonation Engine," AIAA Paper 2019-1253. Doi: 10.2514/6.2019-1253.
- [7] R. Huff, M.D. Polanka, M.J. McClearn, F.R. Schauer, M.L. Fotia, J.L. Hoke, "Design and Operation of a Radial Rotating Detonation Engine," *J. of Propuls. and Power*, 35, 6 (Nov.-Dec. 2019) 1143-1150. Doi: 10.2514/1.B37578.
- [8] A.K. Hayashi, N. Tsuboi, K. Ozawa, T. Watanabe, N.H. Jourdain, K. Ishii, H. Kawana, W. Kuwata, K. Ohno, T. Obara, S. Maeda, E. Dzieminska, X. Tang, T. Mizukaki, "Recent Experimental and Numerical Study on Disc-Type RDEs, AIAA Paper 2020-1169. Doi: 10.2514/6.2019-1169.
- [9] T. Watanabe, K. Shimomura, N.H. Jourdain, T. Kojima, K. Ishii, A.K. Hayashi, "Numerical Simulation on Disk Rotating Detonation Engine: Influence of Internal Flow Field Structure on Performance," AIAA Paper 2020-2160. Doi: 10.2514/6.2020-2160.
- [10] D.E. Paxson, "Preliminary Computational Assessment of Disk Rotating Detonation Engine Configurations," AIAA Paper 2020-2157. Doi: 10.2514/6.2020-2157.
- [11] K. Muraleetharan, M.C. Polanka, F.R. Schauer, R. Huff, "Detonation Confinement using a Flat Channel Plate in a Radial Rotating Detonation Engine," AIAA Paper 2020-0200. Doi: 10.2514/6.2020-0200. .
- [12] N. Tsuboi, Y. Watanabe, T. Kojima, A.K. Hayashi, *Proc. of the Combustion Institute* 35, (2015) 2005-2013.
- [13] T. Yamada, A.K. Hayashi, E. Yamada, N.Tsuboi, V.E. Tangilara, T. Fujiwara, *Comb. Sci. Tech.* 182, (2010) 1901-1914.
- [14] S.A. Zhdan, F.A. Bykovskii, E.F. Vedernikov, *Explosion and Shock Waves* 43, (2007) 449-459.